Appears in the Proceedings of IEEE SPAWC'07, June 2007.

A Three Dimensional Model for Time-Varying Wideband MIMO Mobile-to-Mobile Channels

Alenka G. Zajić and Gordon L. Stüber
School of Electrical and Computer Engineering
Georgia Institute of Technology, Atlanta, GA 30332 USA

***Abstract*— A three-dimensional (3-D) geometrical propagation model for wideband multiple-input multiple-output (MIMO) mobile-to-mobile (M-to-M) communications is proposed. Based on the geometrical model, a 3-D reference model for wideband MIMO M-to-M multipath fading channels is proposed. From the reference model, a space-time-frequency correlation function is derived for a 3-D non-isotropic scattering environment. Finally, it is shown that the time dispersion and the frequency dispersion of a wide sense stationary uncorrelated scattering (WSSUS) channel can not be treated independently, contrary to common practice.**

I. Introduction

Mobile-to-mobile (M-to-M) radio propagation channels arise in inter-vehicular communications, mobile ad-hoc wireless networks, and relay-based cellular radio networks. The statistical properties of M-to-M channels are quite different from conventional fixed-to-mobile (F-to-M) cellular land mobile radio channels [1], [2]. M-to-M communication systems are equipped with low elevation antennas and have both the transmitter ($\mathrm{T_x}$) and receiver ($\mathrm{R_x}$) in motion. Akki and Haber [1], [2] proposed a reference model for SISO M-to-M Rayleigh fading channels. Simulation models for SISO M-to-M channels have been proposed in [3]-[5]. The reference models for narrowband multiple-input multiple-output (MIMO) M-to-M channels have been proposed in [6], [7]. Simulation models for MIMO M-to-M channels have been proposed in [8], [9]. All these models assume that the field incident on the $\mathrm{T_x}$ or $\mathrm{R_x}$ antenna is composed of a number of waves travelling only in the *horizontal* plane. This assumption is acceptable only for certain environments, e.g., rural areas. However, it does not seem appropriate for urban environment in which the $\mathrm{T_x}$ and $\mathrm{R_x}$ antenna arrays are often located in close proximity to and lower than surrounding buildings. Recently, we proposed a three-dimensional (3-D) reference model for *narrowband* MIMO M-to-M multipath fading channels [10].

This article presents a 3-D mathematical reference model for *wideband* MIMO M-to-M channels. To describe our 3-D reference model, we first introduce a 3-D geometrical model for wideband MIMO M-to-M channels, referred to as a concentric-cylinders model. This model is extension of the two-cylinder model for M-to-M channels proposed in [10]. From the 3-D reference model, we derive a space-time-frequency correlation function for a 3-D non-isotropic scattering environment. We present some simulation results to show that the time dispersion and the frequency dispersion of the wide sense stationary uncorrelated scattering (WSSUS) channel can not be treated independently. Finally, we present some simulation results for the space-Doppler power spectral density and compare them with measured data to verify theoretical derivations.

The remainder of the paper is organized as follows. Section II introduces a geometrical concentric-cylinders model. Section III presents a 3-D reference model for wideband MIMO M-to-M channels. Section IV derives the space-time-frequency correlation function for 3-D non-isotropic scattering. Section V presents some simulation and measured results to verify theoretical derivations. Finally, Section VI provides some concluding remarks.

II. A Geometrical Concentric-Cylinders Model

In this section, we introduce a 3-D geometrical model for wideband MIMO M-to-M channels, called a concentric-cylinders model. The concentric-cylinders model is an extension of the two-cylinder model for narrowband M-to-M channels proposed in [10]. We consider a wideband MIMO communication system with L_t transmit and L_r receive omnidirectional antenna elements. It is assumed that both the $\mathrm{T_x}$ and $\mathrm{R_x}$ are in motion and equipped with low elevation antennas. The radio propagation environment is characterized by 3-D wide sense stationary uncorrelated scattering (WSSUS) with non-line-of-sight (NLoS) propagation conditions between the $\mathrm{T_x}$ and $\mathrm{R_x}$.

Fig. 1 shows the concentric-cylinders model for a wideband MIMO M-to-M channel with $L_t = L_r = 2$ antenna elements. The concentric-cylinders model defines four cylinders, two around the $\mathrm{T_x}$ and another two around the $\mathrm{R_x}$, as shown in Fig. 1. Around the transmitter, M fixed omnidirectional scatterers occupy a volume between cylinders of radii R_{t1} and R_{t2}. It is assumed that the M scatterers lie on L cylindric surfaces of radii $R_{t1} \leq R_t^{(l)} \leq R_{t2}$, where $1 \leq l \leq L$. The l^{th} cylindric surface contains $M^{(l)}$ fixed omnidirectional scatterers, and the $(m,l)^{th}$ transmit scatterer is denoted by $S_T^{(m,l)}$. Similarly, around the receiver, N fixed omnidirectional scatterers occupy a volume between cylinders of radii R_{r1} and R_{r2}. It is assumed that N scatterers lie on K cylindric surfaces of radii $R_{r1} \leq R_r^{(k)} \leq R_{r2}$, where $1 \leq k \leq K$.

Prepared through collaborative participation in the Collaborative Technology Alliance for Communications & Networks sponsored by the U.S. Army Research Laboratory under Cooperative Agreement DAAD19-01-2-0011. The U.S. Government is authorized to reproduce and distribute reprints for Government purposes notwithstanding any copyright notation thereon.

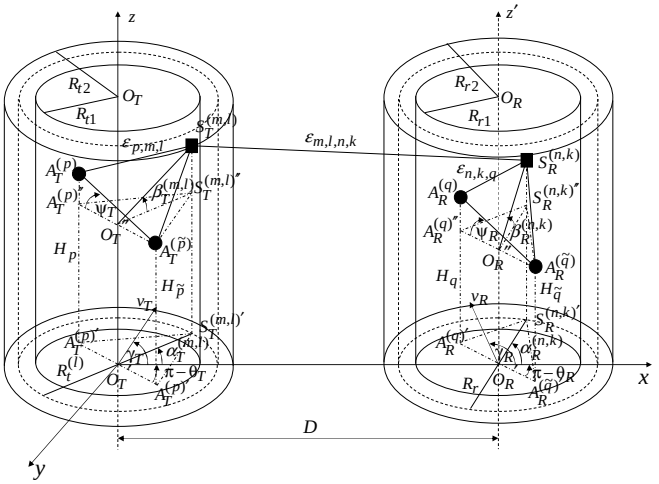

Fig. 1. The concentric-cylinders model for wideband MIMO M-to-M channel with $L_t = L_r = 2$ antenna elements.

The k^{th} cylindric surface contains $N^{(k)}$ fixed omnidirectional scatterers, and the $(n,k)^{th}$ receive scatterer is denoted by $S_R^{(n,k)}$. The distance between the centers of the $\mathrm{T_x}$ and $\mathrm{R_x}$ cylinders is D. It is assumed that the radii R_{t2} and R_{r2} are much smaller than the distance D, i.e., $\max\{R_{t2}, R_{r2}\} \ll D$ (local scattering condition). Furthermore, it is assumed that the distance D is smaller than $4R_{t1}R_{r1}L_r/(\lambda(L_t-1)(L_r-1))$ (channel does not experience keyhole behavior [11]), where λ denotes the carrier wavelength. The spacing between antenna elements at the $\mathrm{T_x}$ and $\mathrm{R_x}$ is denoted by d_T and d_R, respectively. It is assumed that d_T and d_R are much smaller than the radii R_{t1} and R_{r1}, i.e., $\max\{d_T, d_R\} \ll \min\{R_{t1}, R_{r1}\}$. Angles θ_T and θ_R describe the orientation of the $\mathrm{T_x}$ and $\mathrm{R_x}$ antenna array in the x-y plane, respectively, relative to the x-axis. Similarly, angles ψ_T and ψ_R describe the elevation of the $\mathrm{T_x}$'s antenna array and the $\mathrm{R_x}$'s antenna array relative to the x-y plane, respectively. The $\mathrm{T_x}$ and $\mathrm{R_x}$ are moving with speeds v_T and v_R in directions described by angles γ_T and γ_R, respectively. The symbols $\alpha_T^{(m,l)}$ and $\alpha_R^{(n,k)}$ denote the azimuth angle of departure (AAoD) and the azimuth angle of arrival (AAoA), respectively. Similarly, the symbols $\beta_T^{(m,l)}$ and $\beta_R^{(n,k)}$ denote the elevation angle of departure (EAoD) and the elevation angle of arrival (EAoA), respectively. Finally, the symbols $\epsilon_{p,m,l}$, $\epsilon_{m,l,n,k}$, and $\epsilon_{n,k,q}$ denote distances $A_T^{(p)}$ - $S_T^{(m,l)}$, $S_T^{(m,l)}$ - $S_R^{(n,k)}$, and $S_R^{(n,k)}$ - $A_R^{(q)}$, respectively, as shown in Fig. 1.

III. A 3-D Reference Model for Wideband MIMO Mobile-to-Mobile Channels

In this section, we derive a reference model for wideband MIMO M-to-M multipath fading channels. The MIMO channel is described by an $L_r \times L_t$ matrix $\mathbf{H}(t,\tau) = [h_{ij}(t,\tau)]_{L_r \times L_t}$ of the input delay-spread functions. In the 3-D reference model, the number of local scatterers around the $\mathrm{T_x}$ and $\mathrm{R_x}$ is infinite. Consequently, the input delay-spread function of the link $A_T^{(p)} - A_R^{(q)}$ is

$$h_{pq}(t,\tau) = \lim_{M,N\to\infty} \sum_{l,m=1}^{L,M^{(l)}} \sum_{k,n=1}^{K,N^{(k)}} \eta_{l,k}\, g_{m,l,n,k}(t)\, \delta(\tau - \tau_{m,l,n,k}), \quad (1)$$

where parameters $\eta_{l,k}$, $\tau_{m,l,n,k}$ denote amplitudes of the multipath components and time delays, respectively. Function $g_{m,l,n,k}(t)$ is defined as follows

$$\begin{aligned} g_{m,l,n,k}(t) &= e^{-j\frac{2\pi}{\lambda}(\epsilon_{p,m,l}+\epsilon_{m,l,n,k}+\epsilon_{n,k,q})+j\phi_{m,l,n,k}} \quad (2)\\ &\times\ e^{j2\pi t[f_{T\max}\cos(\alpha_T^{(m,l)}-\gamma_T)+f_{R\max}\cos(\alpha_R^{(n,k)}-\gamma_R)]}, \end{aligned}$$

where $f_{T\max} = v_T/\lambda$ and $f_{R\max} = v_R/\lambda$ are the maximum Doppler frequencies associated with the $\mathrm{T_x}$ and $\mathrm{R_x}$, respectively, and λ is the carrier wavelength. The amplitude of the multipath component, $\eta_{l,k}$, is approximated as

$$\eta_{l,k} \approx \frac{\Omega_{pq}}{\sqrt{MN}}\left(1 - \frac{\gamma}{2}\frac{R_t^{(l)} + R_r^{(k)}}{2D}\right), \quad (3)$$

where $\Omega_{pq} = D^{-\gamma/2}\sqrt{P_{pq}}\lambda/4\pi$, P_{pq} is the power transmitted through the subchannel $A_T^{(p)} - A_R^{(q)}$, and γ is the path loss exponent. Finally, the time delay $\tau_{m,l,n,k}$ is defined as the travel time of the wave impinged on the scatterer $S_T^{(m,l)}$ and scattered from the scatterer $S_R^{(n,k)}$, i.e. $\tau_{m,l,n,k} = D/c_0 + R_t^{(l)}(1 - \cos\alpha_T^{(m,l)})/c_0\cos\beta_T^{(m,l)} + R_r^{(k)}(1+\cos\alpha_R^{(n,k)})/c_0\cos\beta_R^{(n,k)}$, where c_0 is the speed of light. It is assumed that the angles of departures (AAoDs and EAoDs), the angles of arrivals (AAoAs and EAoAs), and the radii $R_t^{(l)}$ and $R_r^{(k)}$ are random variables, and that the angles of departure and radii $R_t^{(l)}$ are independent from the angles of arrival and radii $R_r^{(k)}$. Additionally, it is assumed that the phases ϕ_{mn} are random variables uniformly distributed on the interval $[-\pi, \pi)$ and independent form the angles of departure, the angles of arrival, and the radii of the cylinders.

The distances $\epsilon_{p,m,l}$, $\epsilon_{m,l,n,k}$, and $\epsilon_{n,k,q}$ can be expressed as functions of the random variables $\alpha_T^{(m,l)}$, $\alpha_R^{(n,k)}$, $\beta_T^{(m,l)}$, $\beta_R^{(n,k)}$, $R_t^{(l)}$, and $R_r^{(k)}$ as follows:

$$\begin{aligned} \epsilon_{p,m,l} \approx R_t^{(l)} - (0.5L_t + 0.5 - p)\big[&d_{Tz}\sin\beta_T^{(m,l)} + \quad (4)\\ &d_{Tx}\cos\alpha_T^{(m,l)}\cos\beta_T^{(m,l)} + d_{Ty}\sin\alpha_T^{(m,l)}\cos\beta_T^{(m,l)}\big], \end{aligned}$$

$$\begin{aligned} \epsilon_{n,k,q} \approx R_r^{(k)} - (0.5L_r + 0.5 - q)\big[&d_{Rz}\sin\beta_R^{(n,k)} + \quad (5)\\ &d_{Rx}\cos\alpha_R^{(n,k)}\cos\beta_R^{(n,k)} + d_{Ry}\sin\alpha_R^{(n,k)}\cos\beta_R^{(n,k)}\big], \end{aligned}$$

$$\epsilon_{m,l,n,k} \approx D, \quad (6)$$

where $d_{Tx} = d_T\cos\psi_T\cos\theta_T$, $d_{Ty} = d_T\cos\psi_T\sin\theta_T$, $d_{Rx} = d_R\cos\psi_R\cos\theta_R$, $d_{Ry} = d_R\cos\psi_R\sin\theta_R$, $d_{Tz} = d_T\sin\psi_T$, $d_{Rz} = d_R\sin\psi_R$, $p \in \{1,\ldots,L_t\}$, and $q \in \{1,\ldots,L_r\}$. Derivations of expressions (4) - (6) are omitted for brevity.

To simplify further derivations, we will use the time-variant transfer function instead of the input delay-spread function. The time-variant transfer function is defined as the Fourier

transformation of the input delay-spread function and, using (2) - (6), can be written as

$$T_{pq}(t,f)=\mathcal{F}_\tau\left\{h_{pq}(t,\tau)\right\}=\lim_{M,N\to\infty}\sum_{l,m=1}^{L,M^{(l)}}\sum_{k,n=1}^{K,N^{(k)}}\frac{\Omega_{pq}}{\sqrt{MN}}$$
$$\left(1-\frac{\gamma}{2}\frac{R_t^{(l)}+R_r^{(k)}}{2D}\right)a_{p,m,l}b_{q,n,k}e^{-j2\pi fD/c_0+j\phi_{m,l,n,k}}$$
$$e^{j2\pi t[f_{T\max}\cos(\alpha_T^{(m,l)}-\gamma_T)+f_{R\max}\cos(\alpha_R^{(n,k)}-\gamma_R)]} \quad (7)$$
$$e^{-j\frac{2\pi}{c_0}f\left[\frac{R_t^{(l)}}{\cos\beta_T^{(m,l)}}\ 1-\cos\alpha_T^{(m,l)}\ +\frac{R_r^{(k)}}{\cos\beta_R^{(n,k)}}\ 1+\cos\alpha_R^{(n,k)}\right]},$$

where parameters $a_{p,m,l}$ and $b_{q,n,k}$ are defined as

$$a_{p,m,l}=e^{j\frac{\pi}{\lambda}(L_t+1-2p)d_{Tx}\cos\alpha_T^{(m,l)}\cos\beta_T^{(m,l)}-j\frac{2\pi}{\lambda}\ D/2+R_t^{(l)}}$$
$$\times e^{j\frac{\pi}{\lambda}(L_t+1-2p)[d_{Ty}\sin\alpha_T^{(m,l)}\cos\beta_T^{(m,l)}+d_{Tz}\sin\beta_T^{(m,l)}]}, \quad (8)$$
$$b_{q,n,k}=e^{j\frac{\pi}{\lambda}(L_r+1-2q)d_{Rx}\cos\alpha_R^{(n,k)}\cos\beta_R^{(n,k)}-j\frac{2\pi}{\lambda}\left(D/2+R_r^{(k)}\right)}$$
$$\times e^{j\frac{\pi}{\lambda}(L_r+1-2q)[d_{Ry}\sin\alpha_R^{(n,k)}\cos\beta_R^{(n,k)}+d_{Rz}\sin\beta_R^{(n,k)}]}. \quad (9)$$

IV. Space-Time-Frequency Correlation Function of the 3-D Reference Model

Assuming a 3-D non-isotropic scattering environment, we now derive the space-time-frequency correlation function of the 3-D reference model. The normalized space-time-frequency correlation function between two time-variant transfer functions $T_{pq}(t,f)$ and $T_{\tilde{p}\tilde{q}}(t,f)$ is defined as

$$R_{pq,\tilde{p}\tilde{q}}[\Delta t,\Delta f]=\frac{\mathrm{E}\left[T_{pq}(t,f)T^*_{\tilde{p}\tilde{q}}(t+\Delta t,f+\Delta f)\right]}{\sqrt{\mathrm{E}[|T_{pq}(t,f)|^2]\mathrm{E}[|T_{\tilde{p}\tilde{q}}(t,f)|^2]}}, \quad (10)$$

where $(\ \cdot\ )^*$ denotes complex conjugate operation, $\mathrm{E}[\ \cdot\ ]$ is the statistical expectation operator, $p,\tilde{p}\in\{1,\ldots,L_t\}$, and $q,\tilde{q}\in\{1,\ldots,L_r\}$. Using (7) and (10), the space-time-frequency correlation function can be written as

$$R_{pq,\tilde{p}\tilde{q}}[d_T,d_R,\Delta t,\Delta f]=\lim_{M,N\to\infty}\sum_{l,m=1}^{L,M^{(l)}}\sum_{k,n=1}^{K,N^{(k)}} \quad (11)$$
$$\frac{1}{MN}\mathrm{E}\Bigg[\left(1-\gamma\frac{R_t^{(l)}+R_r^{(k)}}{2D}\right)a_{p,m,l}b_{q,n,k}a^*_{\tilde{p},m,l}b^*_{\tilde{q},n,k}$$
$$e^{-j2\pi\Delta t\ \ f_{T\max}\cos(\alpha_T^{(m,l)}-\gamma_T)+f_{R\max}\cos(\alpha_R^{(n,k)}-\gamma_R)}$$
$$e^{j\frac{2\pi}{c_0}\Delta f\left\{D+\frac{R_t^{(l)}}{\cos\beta_T^{(m,l)}}\ 1-\cos\alpha_T^{(m,l)}\ +\frac{R_r^{(k)}}{\cos\beta_R^{(n,k)}}\ 1+\cos\alpha_R^{(n,k)}\right\}}\Bigg].$$

Since the number of local scatterers in the reference model described in Section III is infinite, the discrete AAoDs, $\alpha_T^{(m,l)}$, EAoDs, $\beta_T^{(m,l)}$, AAoAs, $\alpha_R^{(n,k)}$, EAoAs, $\beta_R^{(n,k)}$, and radii $R_t^{(l)}$ and $R_r^{(k)}$ can be replaced with continuous random variables α_T, β_T, α_R, β_R, R_t, and R_r with probability density functions (pdf) $f(\alpha_T,R_t)$, $f(\beta_T)$, $f(\alpha_R,R_r)$, and $f(\beta_R)$, respectively.

In this paper, we assume that the scatterers in the x - y plane are uniformly distributed between the concentric circles of radii R_1 and R_2, i.e.,

$$f(\alpha,R)=\frac{R}{\pi(R_2^2-R_1^2)}. \quad (12)$$

From (12), by calculating marginal probability density functions, we obtain expressions for the pdfs of the azimuth angles and radii as $f(\alpha)=1/2\pi$ and $f(R)=2R/\pi(R_2^2-R_1^2)$, respectively. To characterize the continuous random variables β_T and β_R, we use the pdf [12]

$$f(\varphi)=\begin{cases}\frac{\pi}{4|\varphi_m|}\cos\left(\frac{\pi}{2}\frac{\varphi}{\varphi_m}\right) & ,\ \ |\ \varphi\ |\leq|\ \varphi_m\ |\leq\frac{\pi}{2}\\ 0 & ,\ \ \text{otherwise}\end{cases}, \quad (13)$$

where φ_m is the maximum elevation angle and takes values in the range $10^\circ\leq|\ \varphi_m\ |\leq 20^\circ$ [13]. Note that such elevation angles are typical for M-to-M communications.

By denoting pdf for the $\mathrm{T_x}$ and $\mathrm{R_x}$ radii as $f(R_t)=2R_t/(R_{t2}^2-R_{t1}^2)$ and $f(R_r)=2R_r/(R_{r2}^2-R_{r1}^2)$, and by denoting the pdf for the $\mathrm{T_x}$ and $\mathrm{R_x}$ elevation angles as $f(\beta_T)=\pi\cos(\pi\beta_T/(2\beta_{T_m}))/(4|\beta_{T_m}|)$ and $f(\beta_R)=\pi\cos(\pi\beta_R/(2\beta_{R_m}))/(4|\beta_{R_m}|)$, respectively, the space-time-frequency correlation function in (11) becomes

$$R_{pq,\tilde{p}\tilde{q}}[d_T,d_R,\Delta t,\Delta f]=\int_{R_{t1}}^{R_{t2}}\int_{-\beta_{T_m}}^{\beta_{T_m}}\int_{-\pi}^{\pi}p(\alpha_T,\beta_T,R_t)d\alpha_T d\beta_T dR_t$$
$$\int_{R_{r1}}^{R_{r2}}\int_{-\beta_{R_m}}^{\beta_{R_m}}\int_{-\pi}^{\pi}\left(\frac{1}{2}-\gamma\frac{R_r}{2D}\right)p(\alpha_R,\beta_R,R_r)d\alpha_R d\beta_R dR_r+$$
$$\int_{R_{t1}}^{R_{t2}}\int_{-\beta_{T_m}}^{\beta_{T_m}}\int_{-\pi}^{\pi}\left(\frac{1}{2}-\gamma\frac{R_t}{2D}\right)p(\alpha_T,\beta_T,R_t)d\alpha_T d\beta_T dR_t$$
$$\int_{R_{r1}}^{R_{r2}}\int_{-\beta_{R_m}}^{\beta_{R_m}}\int_{-\pi}^{\pi}p(\alpha_R,\beta_R,R_r)d\alpha_R d\beta_R dR_r, \quad (14)$$

where $p(\alpha_T,\beta_T,R_t)$ and $p(\alpha_R,\beta_R,R_r)$ are defined as

$$p(\alpha_T,\beta_T,R_t)=\frac{\pi}{4|\beta_{T_m}|}\cos\left(\frac{\pi}{2}\frac{\beta_T}{\beta_{T_m}}\right)\frac{R_t}{\pi(R_{t2}^2-R_{t1}^2)}$$
$$e^{j\frac{2\pi}{c_0}\Delta f[D/2+R_t(1-\cos\alpha_T)/\cos\beta_T]}e^{-j2\pi\Delta t f_{T\max}\cos(\alpha_T-\gamma_T)} \quad (15)$$
$$e^{j\frac{2\pi}{\lambda}(\tilde{p}-p)d_T[\cos\psi_T\cos\beta_T(\cos\theta_T\cos\alpha_T+\sin\theta_T\sin\alpha_T)+\sin\psi_T\sin\beta_T]}$$
$$p(\alpha_R,\beta_R,R_r)=\frac{\pi}{4|\beta_{R_m}|}\cos\left(\frac{\pi}{2}\frac{\beta_R}{\beta_{R_m}}\right)\frac{R_r}{\pi(R_{r2}^2-R_{r1}^2)}$$
$$e^{j\frac{2\pi}{c_0}\Delta f[D/2+R_r(1+\cos\alpha_R)/\cos\beta_R]}e^{-j2\pi\Delta t f_{R\max}\cos(\alpha_R-\gamma_R)} \quad (16)$$
$$e^{j\frac{2\pi}{\lambda}(\tilde{q}-q)d_R[\cos\psi_R\cos\beta_R(\cos\theta_R\cos\alpha_R+\sin\theta_R\sin\alpha_R)+\sin\psi_R\sin\beta_R]},$$

respectively. Using trigonometric transformations, the equality $\int_{-\pi}^{\pi}\exp\{ja\sin(c)+jb\cos(c)\}dc=2\pi J_0\left(\sqrt{a^2+b^2}\right)$ [14, eq. 3.338-4], and the results in [10], the space-time-frequency correlation function in (14) can be closely approximated as

$$R_{pq,\tilde{p}\tilde{q}}[d_T,d_R,\Delta t,\Delta f]\approx \quad (17)$$
$$A_T\int_{R_{t1}}^{R_{t2}}e^{j\frac{2\pi}{c_0}\Delta f R_t}J_0\left(\sqrt{x^2+y^2}\right)\frac{2R_t}{R_{t2}^2-R_{t1}^2}dR_t$$
$$A_R\int_{R_{r1}}^{R_{r2}}\left(1-\gamma\frac{R_r}{D}\right)e^{j\frac{2\pi}{c_0}\Delta f R_r}\frac{J_0\left(\sqrt{w^2+z^2}\right)R_r}{R_{r2}^2-R_{r1}^2}dR_r+$$
$$A_T\int_{R_{t1}}^{R_{t2}}\left(1-\gamma\frac{R_t}{D}\right)e^{j\frac{2\pi}{c_0}\Delta f R_t}\frac{J_0\left(\sqrt{x^2+y^2}\right)R_t}{R_{t2}^2-R_{t1}^2}dR_t$$
$$A_R\int_{R_{r1}}^{R_{r2}}e^{j\frac{2\pi}{c_0}\Delta f R_r}J_0\left(\sqrt{w^2+z^2}\right)\frac{2R_r}{R_{r2}^2-R_{r1}^2}dR_r,$$

where parameters A_T, A_R, x, y, z, and w are

$$\begin{aligned}
A_T &= e^{j2\pi\Delta f D/2c_0}\frac{\cos(2\pi\beta_{T_m}(\tilde{p}-p)d_{T_z}/\lambda)}{[1-(4\beta_{T_m}(\tilde{p}-p)d_{T_z}/\lambda)^2]}, \quad (18)\\
A_R &= e^{j2\pi\Delta f D/2c_0}\frac{\cos(2\pi\beta_{R_m}(\tilde{q}-q)d_{R_z}/\lambda)}{[1-(4\beta_{R_m}(\tilde{q}-q)d_{R_z}/\lambda)^2]},\\
x &= j\frac{2\pi}{\lambda}(\tilde{p}-p)d_{T_x}-j2\pi\Delta t f_{T\max}\cos\gamma_T-j\frac{2\pi\Delta f}{c_0}R_t,\\
y &= j\frac{2\pi}{\lambda}(\tilde{p}-p)d_{T_y}-j2\pi\Delta t f_{T\max}\sin\gamma_T,\\
z &= j\frac{2\pi}{\lambda}(\tilde{q}-q)d_{R_x}-j2\pi\Delta t f_{R\max}\cos\gamma_R+j\frac{2\pi\Delta f}{c_0}R_r,\\
w &= j\frac{2\pi}{\lambda}(\tilde{q}-q)d_{R_y}-j2\pi\Delta t f_{R\max}\sin\gamma_R.
\end{aligned}$$

To obtain the space-time-frequency correlation function for the 3-D MIMO M-to-M system, the integrals in (17) must be evaluated numerically, because they do not have closed-form solutions.

In the literature, it is often assumed that the time dispersion (which depends on the scatterer distribution) and the frequency dispersion (which depends on the relative motion between the $\mathrm{T_x}$ and $\mathrm{R_x}$) of a WSSUS channel are statistically independent [15] - [17]. Then, the space-time-frequency correlation function can be factored as [17]

$$\begin{aligned}
R_{pq,\tilde{p}\tilde{q}}[d_T,d_R,\Delta t,\Delta f] &= \quad (19)\\
&R_{pq,\tilde{p}\tilde{q}}[d_T,d_R,\Delta t]R_{pq,\tilde{p}\tilde{q}}[\Delta f].
\end{aligned}$$

Our 3-D reference model will satisfy this assumption iff all scatterers lying on the same cylindric surface have equal time delays, i.e., $\tau_{m,l,n,k}=\tau_{l,k}$. Then, the space-time-frequency correlation function can be written as

$$\begin{aligned}
&R_{pq,\tilde{p}\tilde{q}}[d_T,d_R,\Delta t]R_{pq,\tilde{p}\tilde{q}}[\Delta f]\approx \quad (20)\\
&A_T J_0\left(\sqrt{x_1^2+y_1^2}\right)\int_{R_{t1}}^{R_{t2}} e^{j\frac{2\pi}{c_0}\Delta f R_t}\frac{2R_t}{R_{t2}^2-R_{t1}^2}dR_t\\
&A_R J_0\left(\sqrt{w_1^2+z_1^2}\right)\int_{R_{r1}}^{R_{r2}}\left(1-\gamma\frac{R_r}{D}\right)\frac{e^{j\frac{2\pi}{c_0}\Delta f R_r}R_r}{R_{r2}^2-R_{r1}^2}dR_r+\\
&A_T J_0\left(\sqrt{x_1^2+y_1^2}\right)\int_{R_{t1}}^{R_{t2}}\left(1-\gamma\frac{R_t}{D}\right)\frac{e^{j\frac{2\pi}{c_0}\Delta f R_t}R_t}{R_{t2}^2-R_{t1}^2}dR_t\\
&A_R J_0\left(\sqrt{w_1^2+z_1^2}\right)\int_{R_{r1}}^{R_{r2}} e^{j\frac{2\pi}{c_0}\Delta f R_r}\frac{2R_r}{R_{r2}^2-R_{r1}^2}dR_r,
\end{aligned}$$

where $x_1=j2\pi(\tilde{p}-p)d_{T_x}/\lambda-j2\pi\Delta t f_{T\max}\cos\gamma_T$, $y_1=j2\pi(\tilde{p}-p)d_{T_y}/\lambda-j2\pi\Delta t f_{T\max}\sin\gamma_T$, $z_1=j2\pi(\tilde{q}-q)d_{R_x}/\lambda-j2\pi\Delta t f_{R\max}\cos\gamma_R$, and $w_1=j2\pi(\tilde{q}-q)d_{R_y}/\lambda-j2\pi\Delta t f_{R\max}\sin\gamma_R$. Finally, solving the integrals in (20), the space-time-frequency correlation function becomes

$$\begin{aligned}
&R_{pq,\tilde{p}\tilde{q}}[d_T,d_R,\Delta t]R_{pq,\tilde{p}\tilde{q}}[\Delta f]\approx \quad (21)\\
&A_T A_R J_0\left(\sqrt{x_1^2+y_1^2}\right)J_0\left(\sqrt{w_1^2+z_1^2}\right)(I_{T1}I_{R2}+I_{T2}I_{R1}),
\end{aligned}$$

where $I_{T1}=2(e^{jaR_{t2}}(1-jaR_{t2})-e^{jaR_{t1}}(1-jaR_{t1}))/a^2b_t$, $I_{R1}=2(e^{jaR_{r2}}(1-jaR_{r2})-e^{jaR_{r1}}(1-jaR_{r1}))/a^2b_r$, $I_{T2}=(e^{jaR_{t2}}(-2jc-ja^2R_{t2}+a-2caR_{t2}+jca^2R_{t2}^2)-e^{jaR_{t1}}(-2jc-ja^2R_{t1}+a-2caR_{t1}+jca^2R_{t1}^2)/a^3b_t$, $I_{R2}=(e^{jaR_{r2}}(-2jc-ja^2R_{r2}+a-2caR_{r2}+jca^2R_{r2}^2)-e^{jaR_{r1}}(-2jc-ja^2R_{r1}+a-2caR_{r1}+jca^2R_{r1}^2)/a^3b_r$, $a=2\pi\Delta f/c_0$, $b_t=R_{t2}^2-R_{t1}^2$, $b_r=R_{r2}^2-R_{r1}^2$, and $c=\gamma/D$.

V. Simulation Results

In this section, we present some simulation and measured results to verify theoretical derivations. In all simulations, we use a normalized sampling period $f_{T\max}T_s=0.01$ ($f_{T\max}=f_{R\max}$ are the maximum Doppler frequencies and T_s is the sampling period). The number of transmit and receive antennas is set to $L_t=L_r=2$. The parameters used to obtain curves in Figs. 2 - 4 are $\beta_{Tm}=\beta_{Rm}=15^\circ$, $\theta_T=\theta_R=\pi/4$, $\psi_T=\psi_R=\pi/3$, $\gamma_T=\gamma_R=20^\circ$, $R_{t1}=R_{r1}=30m$, $R_{t2}=R_{r2}=300m$, $D=5000m$, and $\gamma=4$.

To validate assumptions used to obtain the space-time-frequency correlation function in (21), we compare it with the numerically obtained space-time-frequency correlation function in (17). In Figs. 2 - 4, we compare the space-time correlation functions, the frequency correlation functions, and the space-time-frequency correlation functions in (17) and (21). Fig. 2 shows good agreement between the space-time correlation functions in (17) and (21). Fig. 3 shows relatively

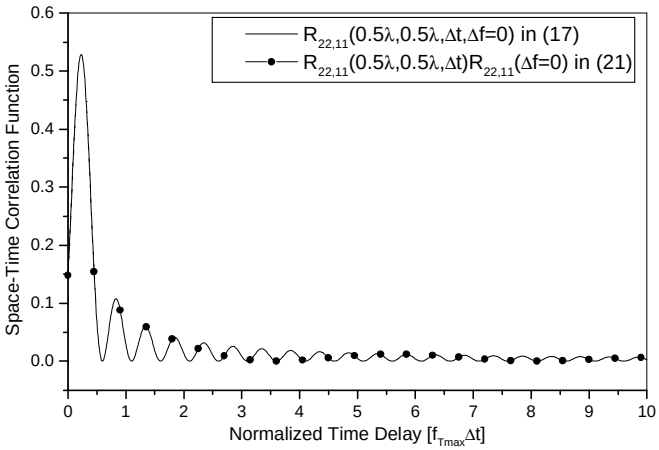

Fig. 2. Comparison of the normalized space-time correlation functions in (17) and (21).

good agreement between the frequency correlation functions in (17) and (21). However, Fig. 4 shows that Eq. (21) underestimates the space-time-frequency correlation and that the time dispersion and the frequency dispersion of the WSSUS channel are not statistically independent. Instead, the numerically obtained space-time-frequency correlation function in (17) should be used. Finally, in Fig. 5 we compare the Doppler spectra obtained using our concentric-cylinders model (for $d_T=d_R=0$) with measured Doppler spectra for SISO system. The measured results are taken from Fig. 4(d) of [18]. The close agreement between the theoretical and empirical curves confirms the utility of the proposed wideband model.

VI. Conclusions

This paper introduced a concentric-cylinders geometrical propagation model. Based on this geometrical model, a 3-D

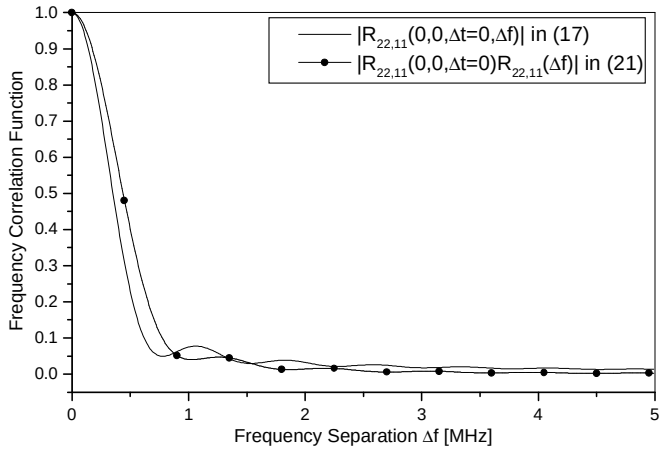

Fig. 3. Comparison of the absolute value of the frequency correlation functions in (17) and (21).

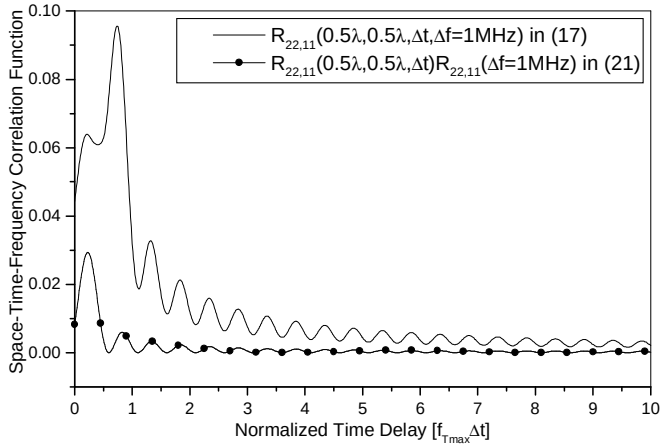

Fig. 4. Comparison of the normalized space-time-frequency correlation functions in (17) and (21).

reference model for wideband MIMO M-to-M fading channels is proposed. From the reference model, a space-time-frequency correlation function for a 3-D non-isotropic scattering environment is derived. Simulation results are presented to verify theoretical derivations. Finally, it is shown that the time and frequency dispersion of the WSSUS channel can not be treated independently, contrary to common practice.

DISCLAIMER

The views and conclusions contained in this document are those of the authors and should not be interpreted as representing the official policies, either expressed or implied, of the Army Research Laboratory or the U. S. Government.

REFERENCES

[1] A.S. Akki and F. Haber, "A statistical model for mobile-to-mobile land communication channel," *IEEE Trans. on Veh. Tech.*, vol. 35, pp. 2–10, Feb. 1986.

[2] A.S. Akki, "Statistical properties of mobile-to-mobile land communication channels," *IEEE Trans. on Veh. Tech.*, vol. 43, pp. 826–831, Nov. 1994.

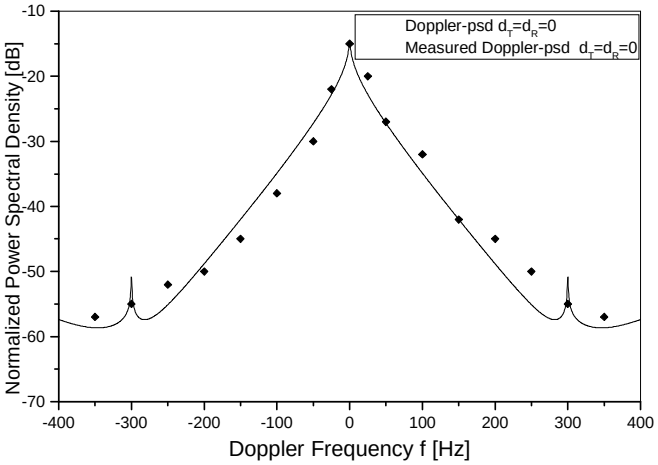

Fig. 5. The normalized simulated and measured Doppler power spectra for SISO system.

[3] R. Wang and D. Cox, "Channel modeling for ad hoc mobile wireless networks," *Proc. IEEE Veh. Tech. Conf.*, vol. 1, pp. 21–25, Birmingham, AL, May 2002.

[4] C.S. Patel, G.L. Stüber, and T. G. Pratt, "Simulation of Rayleigh-faded mobile-to-mobile communication channels," *IEEE Trans. on Commun.*, vol. 53, pp. 1876–1884, Nov. 2005.

[5] A.G. Zajić and G.L. Stüber, "A new simulation model for mobile-to-mobile Rayleigh fading channels," *Proc. IEEE WCNC'06*, Las Vegas, NE, USA, April 2006.

[6] M. Pätzold, B.O. Hogstad, N. Youssef, and D. Kim, "A MIMO mobile-to-mobile channel model: Part I-the reference model," *Proc. IEEE PIMRC'05*, vol. 1, pp. 573–578, Berlin, Germany, Sept. 2005.

[7] A.G. Zajić and G.L. Stüber, "Space-time correlated MIMO mobile-to-mobile channels," *Proc. IEEE PIMRC'06*, Helsinki, Finland, Sept. 2006.

[8] B.O. Hogstad, M. Pätzold, N. Youssef, and D. Kim, "A MIMO mobile-to-mobile channel model: Part II-the simulation model," *Proc. IEEE PIMRC'05*, vol. 1, pp. 562–567, Berlin, Germany, Sept. 2005.

[9] A.G. Zajić and G.L. Stüber, "Simulation models for MIMO mobile-to-mobile channels," *Proc. IEEE MILCOM'06*, Washington, D.C., USA, Oct. 2006.

[10] A.G. Zajić and G.L. Stüber, "A three-dimensional MIMO mobile-to-mobile channel model," *IEEE WCNC'07*, Hong Kong, March 2007.

[11] D. Gesbert, H. Bölcskei, D.A. Gore, and A.J. Paulraj, "Outdoor MIMO wireless channels: models and performance prediction," *IEEE Trans. on Commun.*, vol. 50, pp. 1926–1934, Dec. 2002.

[12] J.D. Parsons and A.M.D. Turkmani, "Characterisation of mobile radio signals: model description," *IEE Proc. I, Commun., Speach, and Vision*, vol. 138, pp. 549–556, Dec. 1991.

[13] A. Kuchar, J.-P. Rossi, and E. Bonek, "Directional macro-cell channel characterization from urban measurements," *IEEE Trans. on Antennas and Propagation*, vol. 48, pp. 137–146, Feb. 2000.

[14] I.S. Gradshteyn and I.M. Ryzhik, *Table of Integrals, Series, and Products* 5^{th} *ed.*. A. Jeffrey, Ed. San Diego CA: Academic, 1994.

[15] K.-W. Yip and T.-S. Ng, "Karhunen-Loève expansion of the WSSUS channel output and its application to efficient simulation," *IEEE Journal on Select. Areas in Commun.*, vol. 15, pp. 640–646, May 1997.

[16] P. Hoeher, "A statistical discrete-time model for the WSSUS multipath channel," *IEEE Trans. on Veh. Tech.*, vol. 41, pp. 461–468, Nov. 1992.

[17] E. Chiavaccini and G.M. Vitetta, "GQR models for multipath Rayleigh fading channels," *IEEE Journal on Select. Areas in Commun.*, vol. 19, pp. 1009–1018, June 2001.

[18] G. Acosta, K. Tokuda, and M. A. Ingram,"Measured joint Doppler-delay power profiles for vehicle-to-vehicle communications at 2.4 GHz," *Proc. IEEE GLOBECOM'04*, vol. 6, pp. 3813–3817, Dallas, TX, Nov. 2004.